Qualitative Measure of Photocurrent Enhancement in Silicon Solar Cells due to Plasmonic Antennas

Nathan Burford[1] and Magda El-Shenawee[2]

[1,2]Computational Electromagnetics Group
[1]Microelectronics-Photonics Program
[2]Department of Electrical Engineering
University of Arkansas, Fayetteville, AR, 72701, United States
nburford@uark.edu, magda@uark.edu

Abstract: This work presents a method for the approximation of photocurrent enhancement in plasmonic solar cells. Nano-toroids are positioned in the top of the silicon substrate. Spectral distribution of the plasmonic induced enhancement of electromagnetic absorption within the silicon layer of a solar cell is computed using Ansys® HFSS. The obtained results are utilized in a qualitative expression to approximate the percent enhancement in the generated photocurrent. Initial results show significant variance in the calculated photocurrent enhancement between plasmonic solar cell designs that is not as pronounced when simply comparing the enhancement of the field absorption in silicon.

Keywords: Plasmons, Computational Electromagnetics, Solar Cells, Photovoltaics, Thin-Films

1. Introduction

The past decade has seen increasing interest in the various applications of nanoplasmonics. Specifically, nanoplasmonics show potential for increasing the collection efficiencies of thin-film photovoltaic devices [1-4]. This is possible through the unique interaction that these nano-scale metallic particles have with light. When exposed to incident electromagnetic radiation at the nano-particles resonant frequency, the electrons within the particle experience a strong oscillation. This allows significant near-field enhancement of the electromagnetic energy around the particle as well as scattering of the transmitted light. This scattering provides the opportunity for transmitted light to be coupled into waveguide modes of the silicon layer, thus trapping the transmitted radiation and greatly increasing the absorption in the silicon [4, 5]. It has been shown previously how shape, size, surface coverage and material properties of these nanoparticles all have a significant effect on the spectral location and strength of the plasmon resonance [6, 7]. As such, optimization of these parameters is needed to determine the nanoparticle shapes and surface coverage that provides the greatest photocurrent enhancement.

Design and optimization of plasmonic nanostructures for photovoltaic applications offers some unique challenges. It has been show extensively how commercially available computational electromagnetic solvers can be utilized to quantify the wavelength dependent plasmonic induced enhancement of electromagnetic fields in the silicon layer [1-4]. However, there is still no direct method for using this information to calculate the theoretical enhancement of the output photocurrent a solar cell would have, and comparison of the spectral distribution of the energy enhancement in the silicon layer does not include many wavelength dependent material properties that will affect the photocurrent enhancement. In this work, a qualitative metric for utilizing the wavelength dependent enhancement of electromagnetic energy in a photovoltaic absorbing layer is presented to approximate the percent enhancement of generated photocurrent. A comparison of this metric between plasmonic solar cell designs is demonstrated.

2. Methodology

A. HFSS Simulation

The first step in comparing designs of plasmonic solar cells is to set up the configuration of the computational domain and define the parameters to be optimized. Fig. 1a illustrates the desired representation, an infinite array of silver nanoparticles equally spaced in a square lattice across the x-y plane atop a silicon layer illuminated by an incident plane wave linearly polarized in the x-direction and propagating in the -z direction. Due to the incident wave having $\vec{E}$ and $\vec{H}$ vectors normal to the x-z and y-z faces, respectively, perfect $\vec{E}$ and perfect $\vec{H}$ symmetry boundaries can be placed at these faces, shown in fig. 1d and 1e respectively. This reduces the simulation domain to 1/4 of the original, as shown in figure 1c, while still emulating an infinite array of nanoparticles. Material electrical parameters are taken from Palik [8].

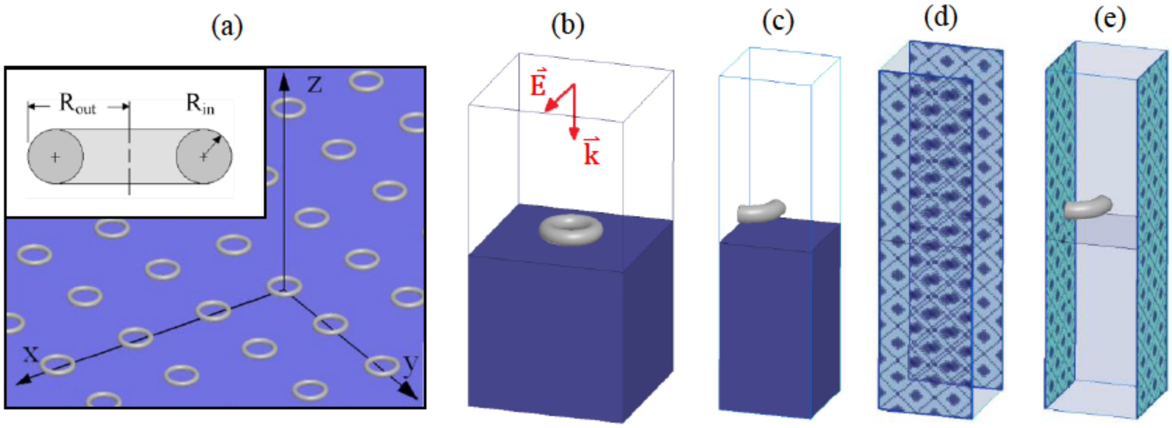

Fig. 1. (a) Illustration of infinite square lattice array of toroid shaped nanoparticles on a silicon substrate. Inset shows definition of toroid geometric parameters R_{out} and R_{in}. (b) Full computational domain, (c) reduced computational domain, (d) perfect electric conductor boundaries and (e) perfect magnetic conductor boundaries.

In order to quantify the wavelength dependent enhancement of transmitted electromagnetic energy in the silicon layer, the absorbed electric fields in the silicon are calculated and integrated across the silicon volume. Taking the ratio of this value for the plasmonic enhanced case and a reference case with no nano-toroids present provides a ratio equivalent to the enhancement of electromagnetic energy within the silicon layer with σ being the conductivity of silicon:

$$\mathrm{EF}(\lambda) = \frac{\int \sigma |\mathbf{E}_{\mathbf{withNPs}}|^2 \mathrm{dV_{Si}}}{\int \sigma |\mathbf{E}_{\mathbf{withoutNPs}}|^2 \mathrm{dV_{Si}}}. \tag{1}$$

B. Approximate Photocurrent Enhancement

Analysis of the spectral resonance response of plasmonic nano-toroids does not provide complete information of enhanced photocurrent generation. Wavelength dependent material parameters of the absorbing layer and the electron-hole pair generating must be coupled with the plasmonic enhancement in order to provide a more accurate comparison between nano-toroids designs. Thus, in order to qualitatively measure the photocurrent enhancement, the wavelength dependent enhancement factor from the computational analysis is used in conjunction with a straightforward calculation to approximate this enhancement in output current density.

Consider first a unit area thin film solar cell of thickness d under incident AM1.5 solar radiation. The spectral distribution of the output current density can be approximated as,

$$\mathrm{J_{ref}}(\lambda) = \mathrm{I_{AM1.5}}(\lambda)[1 - \mathrm{R}(\lambda)]\left[1 - \mathrm{e}^{-\alpha(\lambda)\mathrm{d}}\right] \frac{\lambda}{\mathrm{hc}}\mathrm{q}. \tag{2}$$

Here, $\mathrm{I_{AM1.5}}(\lambda)$ represents the standard AM1.5 solar flux in W/(nm m^2), $\mathrm{R}(\lambda)$ is the wavelength dependent reflection at an air-silicon interface, $1 - \mathrm{e}^{-\alpha(\lambda)\,\mathrm{d}}$ represents the fraction of transmitted solar radiation absorbed within the silicon layer d corresponding to a wavelength dependent silicon absorption coefficient of $\alpha(\lambda)$, λ/hc is the number of photons per incident energy flux of wavelength λ where h is Plank's constant and c is the speed of light in vacuum, and q is the electric charge of a single electron.

Consider the following component of equation (2),

$$[1 - \mathrm{R}(\lambda)]\,\left[1 - \mathrm{e}^{-\alpha(\lambda)\mathrm{d}}\right]. \tag{3}$$

This represents the fraction of incident electromagnetic energy absorbed within a reference solar cell. Since the enhancement factor defined in (1) represents the percent enhancement of electromagnetic energy within the cell, the fraction of absorbed electromagnetic energy for a plasmonic enhanced case can be approximated as,

$$\mathrm{EF}(\lambda)[1 - \mathrm{R}(\lambda)]\left[1 - \mathrm{e}^{-\alpha(\lambda)\mathrm{d}}\right]. \tag{4}$$

As such, the spectral distribution of the output current density for a plasmonic enhanced case will be defined as,

$$\mathrm{J_{NPs}}(\lambda) = \mathrm{I_{AM1.5}}(\lambda)\mathrm{EF}(\lambda)[1 - \mathrm{R}(\lambda)]\left[1 - \mathrm{e}^{-\alpha(\lambda)\mathrm{d}}\right]\frac{\lambda}{\mathrm{hc}}\mathrm{q}. \tag{5}$$

Integration across λ for the spectral distribution of any current density yields a value for the output photocurrent per unit surface area of a solar cell. Thus, integrating (2) and (3) across λ and taking the ratio of these two values provides an approximation of the percent enhancement in output photocurrent generation of a plasmonic solar cell.

$$\%\mathrm{PE} = \frac{\int \mathrm{J_{NPs}}(\lambda)\mathrm{d}\lambda}{\int \mathrm{J_{ref}}(\lambda)\mathrm{d}\lambda} \times 100. \tag{6}$$

Thus, equation (6) provides a qualitative metric for comparing the percent photocurrent enhancement in various designs of plasmonic enhanced solar cells.

There are several approximations this calculation makes. First, it assumes that all absorbed photons with energy greater than the material band gap will produce an electron-hold pair. Second, it assumes that all generated electron-hole pairs will be collected and contribute to the output photocurrent. The third assumption is that the enhancement of electromagnetic field intensity as described in (1) is identical to the enhancement of the photon absorption in the silicon layer, that is, if $|\mathrm{E}|^2$ in the silicon layer is 10% higher at a given wavelength in the plasmonic enhanced case, the number of absorbed photons at that wavelength will also be 10% higher. In calculating the output photocurrent as in (2) and (3), these approximations will lead to a significantly higher value than would occur in reality. However, considering the ratio of photocurrents as in (6) still provides an effective metric for comparing plasmonic solar cell designs without requiring more complicated modeling of the semiconductor device physics.

3. Numerical results

Figure 2 illustrates the HFSS enhancement factor calculations for three preliminary plasmonic solar cell designs utilizing toroid shaped silver nanoparticles. This wavelength dependent enhancement factor is the key component that determines the effectiveness of a particular plasmonic solar cell design. All three maintain an outer radius of 42 nm, 2 nm spacing above the silicon from the bottom of the nanoparticle and 1440 nm spacing between adjacent particles, with the three cases representing variance of the toroid inner radius of 14.5 nm, 13.5 nm and 10.5 nm as defining in fig. 1a. It should be noted that these are not cases in which particle size and spacing have been optimized. These results illustrate the shift in the spectral location of the plasmon resonance of widely spaced nanotoroids as they are made thinner or thicker.

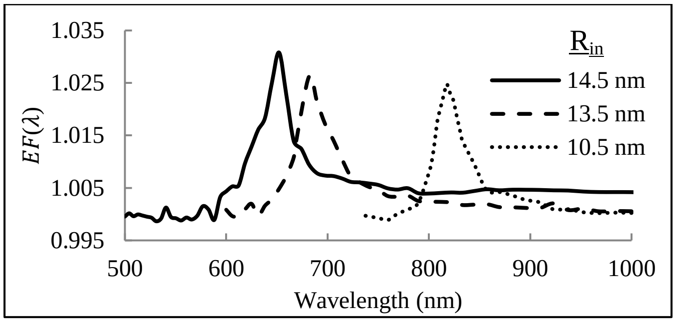

Fig. 2. EF(λ) for silver nanotoroids of R_{in} = 14.5 nm, 13.5 nm and 10.5 nm.

Table 1 shows a comparison of the three designs, including the spectral location of the EF(λ) peak defined as λ_{max}, the maximum value of the peak $EF(\lambda_{max})$ in percent enhancement and the %PE calculated using (6). The maximum values of both $EF(\lambda_{max})$ and %PE are highest for Toroid 1 with $EF(\lambda_{max})$ = 3.08% and %PE = 0.30%. From Toroid 1 to Toroid 2, there is a 15% decrease in$EF(\lambda_{max})$, from 3.08% to 2.62% and a 27% decrease in %PE, from 0.30% to 0.22%. From Toroid 2 to Toroid 3 there is a 6% decrease in$EF(\lambda_{max})$, from 2.62% to 2.47% and an 82% decrease in %PE, 0.22% to 0.04%. What this shows is that the method of simply comparing spectral locations and peaks in EF(λ) does not correlate to the comparison of %PE. The values of %PE for each case vary much more than the maximum values of the EF(λ) peaks due to the wavelength dependent characteristics of the solar cell that are taken into account in (6). It is imperative to note that these designs represent very wide dispersion of nanoparticles with less that 0.3% nanoparticle surface coverage. This is the reason for the low values of %PE for the designs, as previous work in the optimization of spherical silver nanoparticles illustrates maximal enhancement between 5% and 45% surface coverage, depending on nanoparticle size [3]. Thus, by optimizing the surface coverage of these nano-toroids it is expected that much higher photocurrent enhancement can be obtained.

Table 1: Comparison of evaluation metrics for three nanotoroid geometries

	R_{in}	λ_{max}	$EF(\lambda_{max})$	%PE
Toroid 1	14.5 nm	652 nm	3.08%	0.30%
Toroid 2	13.5 nm	682 nm	2.62%	0.22%
Toroid 3	10.5 nm	817 nm	2.47%	0.04%

4. Conclusion

In this work, a simple metric for the approximation of plasmonic photocurrent enhancement in photovoltaic devices is presented. Initial results investigating silver toroid nanoparticle designs have illustrated that there is a significant advantage in this method over simply comparing the spectral distribution of the electromagnetic energy enhancement between nanoparticle designs. The presented metric provides an effective comparative method to use when optimizing plasmonic solar cells. Future work comparing this theoretical method to experimental measurements would provide insight to the validity of the approximations made in this model.

Acknowledgement

This work is supported mainly through the NSF/ECCS award # 1006927 and in part through NSF Cyber infrastructure awards EP-0918970 and MRI # 072265 and NSF GK12 award # 0538645. The authors would like to thank the staff of AHPCC for their technical support.

References

[1] D. Derkacs, S. H. Lim, P. Matheu, W. Mar, and E. T. Yu, “Improved performance of amorphous silicon solar cells via scattering from surface plasmon polaritons in nearby metallic nanoparticles,” *Applied Physics Letters* vol. 89, no. 093103, 2006.
[2] Mokkapati, F. J. Beck, R. de Waele, A. Polman, and K. R. Catchpole, “Resonant nano-antennas for light trapping in plasmonic solar cells,” *J. Phys. D: Appl. Phys*. vol. 44, no. 185101, 2011.
[3] Y. Akimov, W. Koh, “Resonant and nonresonant plasmonic nanoparticle enhancement for thin-film silicon solar cells,” *Nanotechnology*, vol. 21, no. 235201, pp. 1-6, May, 2010.
[4] N. Burford, M. El-Shenawee, S. Shumate, D. Hutchings, H. Naseem, “Field enhancement due to surface structuring during aluminum induced crystallization of amorphous silicon,” *Proc. of the IEEE Int. Symp. on Antennas and Prop. and USNC/URSI National Radio Science Meeting*, Chicago, USA, July 8-13, 2012.
[5] G. Beaucarne, “Silicon thin-film solar cells,” *Advances in OptoElectronics*, vol. 2007, no. 36970, pp. 1-12, Aug. 2007.
[6] M. El-Shenawee, P. Blake, A. M. Hassan, and D. K. Roper, "Surface Plasmons of Finite Nanoring Arrays," *Proc. of the IEEE International Symposium on Antennas and Propagation and USNC/URSI National Radio Science Meeting*, pp. 1609-1612, 2011.
[7] W. Cao, T. Huang, X. Xu, H. Elsayed-Ali, "Localized surface plasmon resonance of single silver nanoparticles studies by dark-field optical microscopy and spectroscopy," *J. Appl. Phys*. vol. 109, no. 034310, pp. 1-6, Feb. 2011.
[8] E. D. Palik, *Handbook of Optical Constants of Solids*, New York: Academic, New York, 1985.